PERGAMON

Vision Research 43 (2003) 683–696

Vision Research

www.elsevier.com/locate/visres

Independence of mechanisms tuned along cardinal and non-cardinal axes of color space: evidence from factor analysis

Karen L. Gunther, Karen R. Dobkins *

Department of Psychology, University of California, San Diego, La Jolla, CA 92093, USA

Received 6 February 2002; received in revised form 18 September 2002

Abstract

Many previous studies employing paradigms such as adaptation, masking and summation-near-threshold have demonstrated the existence of separate mechanisms underlying the detection of the three cardinal axes of color space: $L+M$, $L-M$ and $S-(L+M)$. In addition, some studies have demonstrated the existence of higher-order mechanisms tuned to non-cardinal axes (which are made up of combinations of the cardinal axes). In order to address the issue of separate and independent color mechanisms further, here we applied factor analysis to contrast threshold data obtained from 41 subjects for nine different axes in color space (the three cardinal axes and the six non-cardinal axes midway between). In line with previous studies, the results of a three-factor analysis performed on contrast thresholds for the cardinal axes revealed independence across the three. However, in some of our factor analyses (for example, when a two-factor analysis was performed on the cardinal axes), intercorrelation was observed between $L-M$ and $S-(L+M)$ stimuli. With regard to higher-order mechanisms, our factor analyses revealed mechanisms selective for non-cardinal axes within the $(L-M)/(L+M)$ and $(S-(L+M))/(L+M)$ color planes, but not the $(L-M)/(S-(L+M))$ color plane. To ensure that the intercorrelation observed between $L-M$ and $S-(L+M)$ cardinal axes was not due to the particular stimulus parameters or testing measures employed, in three of our subjects we performed a "summation-near-threshold" experiment using experimental conditions nearly identical to those in the factor analysis experiments. In accordance with previous findings [*Vision Research* 39 (1999) 733], $L-M$ and $S-(L+M)$ stimuli were found to be separable in this analysis. This seeming discrepancy between the results of our factor analysis and those obtained from paradigms such as summation-near-threshold can be resolved by proposing that the mechanisms underlying detection of $L-M$ and $S-(L+M)$ stimuli are *separable* (as defined by the ability to isolate activity within each mechanism using select stimuli), yet nonetheless *intercorrelated*. Such intercorrelation could arise if these two mechanisms are limited by the same source of variability and/or subject to the same gain control.

1. Introduction

Theories of color vision typically posit three postreceptoral mechanisms, which are derived from the sums and differences of the three cone types. One mechanism (often referred to as the "luminance" mechanism) signals a weighted sum of long-wavelength-selective (L) and medium-wavelength-selective (M) cones, i.e., "$L+M$" (with some debate regarding the contribution of short-wavelength-selective (S) cones: Eisner & MacLeod, 1980; Boynton, Eskew, & Olson, 1985; Stockman, MacLeod, & DePriest, 1991). Two chromatic mechanisms signal weighted sums and differences of the cones. The "$L-M$" mechanism signals differences between L- and M-cones (and is often referred to as the "red/green" mechanism). The "$S-(L+M)$" mechanism signals differences between S-cones and the sum of L- and M-cones (and is often referred to as the "blue/yellow" or "tritan" mechanism). The stimuli that activate one of these mechanisms in isolation from the other two are referred to as the *cardinal axes* of color space. Evidence for the existence of three postreceptoral mechanisms has come from several previous psychophysical experiments, using paradigms such as adaptation (Krauskopf, Williams, & Heeley, 1982; Bradley, Switkes, & DeValois, 1988; Webster & Mollon, 1991, 1994; and Krauskopf & Gegenfurtner, 1992), masking (Gegenfurtner & Kiper, 1992; Mullen & Losada, 1994, 1999; Li & Lennie, 1997; Sankeralli & Mullen, 1997; Giulianini & Eskew, 1998; but cf. Switkes, Bradley, & DeValois, 1988), summation-near-threshold (Mullen, Cropper, & Losada, 1997; Mullen & Sankeralli, 1999; but cf. Gur & Akri, 1992), visual search

* Corresponding author. Tel.: +1-858-534-5434.
E-mail address: kdobkins@ucsd.edu (K.R. Dobkins).

0042-6989/03/$ - see front matter
doi:10.1016/S0042-6989(02)00689-2

(Monnier & Nagy, 2001) and motion integration (Krauskopf, Wu, & Farell, 1996).

In addition to investigating the existence of mechanisms tuned for the cardinal axes of color space, other studies have investigated the existence of higher-order color mechanisms sensitive to non-cardinal axes of color space. Because non-cardinal axes are made up of *combinations* of the cardinal axis stimuli, they necessarily activate more than one lower-order mechanism. Thus, mechanisms tuned for non-cardinal axes (should they exist) must receive convergent input from two or more lower-order mechanisms tuned for cardinal axes (and thus originate at a processing stage past where these cardinal axes are first represented). Psychophysical studies investigating the existence of higher-order color mechanisms have yielded somewhat equivocal results, with some studies providing evidence for (Krauskopf, Williams, Mandler, & Brown, 1986; Flanagan, Cavanagh, & Favreau, 1990; Webster & Mollon, 1991, 1994; D'Zmura, 1991; Kooi, DeValois, Switkes, & Grosof, 1992; Krauskopf & Gegenfurtner, 1992; Dobkins, Stoner, & Albright, 1998; D'Zmura & Knoblauch, 1998), and some against (Sankeralli & Mullen, 1997; Giulianini & Eskew, 1998) mechanisms selective for non-cardinal stimuli.

In the present study, we investigated the independence of lower- and higher-order color mechanisms using a factor analytic approach. Recently, we and others have used this technique to demonstrate the independence of contrast detection for two of the three ($L+M$ and $L-M$) cardinal axes in color space (Dobkins, Gunther, & Peterzell, 2000; Peterzell & Teller, 2000; Gunther & Dobkins, 2002). Here, we extend these results by applying factor analysis to contrast threshold data for stimuli modulated along nine axes in color space: the three cardinal axes ($L+M$, $L-M$ and $S-(L+M)$) and the six non-cardinal axes midway between them. The methods and theories underlying the factor analytic approach have been described in detail elsewhere (e.g., Sekuler, Wilson, & Owsley, 1984; Webster & MacLeod, 1988; Peterzell, Werner, & Kaplan, 1993, 1995; and see Peterzell & Teller, 1996 for a non-technical and historical overview of the topic). In brief, this technique uses individual differences across subjects as a means to reveal the number of visual mechanisms underlying performance across a range of stimulus conditions. Specifically, when performance under different stimulus conditions is controlled by a single visual mechanism, subject differences observed under one condition are expected to correlate highly with subject differences in the other conditions. By contrast, when performance under the different conditions is controlled by *independent* mechanisms, no such correlation is expected. Factor analysis applied to correlations in data obtained across a variety of stimulus conditions estimates the number and nature of underlying visual mechanisms. The term "factors" is used to describe visual mechanisms estimated from this procedure, to differentiate them from visual mechanisms derived from other methods.

Using this approach, we predicted that detection of the three cardinal axes would be governed by independent mechanisms, and thus modeled by separate factors. Likewise, if detection of non-cardinal axes is mediated by independent higher-order mechanisms, multiple higher-order factors were also expected to be revealed. To test these hypotheses, we obtained contrast threshold data from 41 subjects for nine axes of color space at each of three spatial frequencies (27 total stimuli). Factor analysis was then applied to the data to investigate the nature of mechanisms underlying the results. In general, the results of these factor analyses revealed the existence of independent mechanisms tuned to cardinal, as well as non-cardinal, axes of color space.

In several of our analyses, however, we observed a tendency for intercorrelation between the $L-M$ and $S-(L+M)$ cardinal axes. In order to ensure that this intercorrelation was not due to the particular stimulus parameters (e.g., spatial/temporal frequency, stimulus size, duration, etc.) or testing measure (i.e., contrast thresholds) employed, we investigated the separability of these cardinal axes using nearly identical stimuli in a summation-near-threshold paradigm. In accordance with previous studies, the results of our summation-near-threshold experiments revealed clear separability between the $L-M$ and $S-(L+M)$ axes. Although this finding may, at first glance, appear to contradict our results obtained using factor analysis, we point out that the results from experiments employing summation-near-threshold (as well as adaptation and masking) are more accurately described as providing evidence for *separability* across mechanisms (as defined by the ability to isolate activity within each mechanism using select stimuli) rather than evidence for *independence* (as defined by a lack of correlation amongst separable mechanisms) *per se*. By these definitions, mechanisms may be separable, yet not entirely independent if, for example, they are limited by the same source of variability or subject to the same gain control. However, mechanisms that exhibit independence should necessarily be separable from one another. Thus, the results of the present factor analyses, taken together with results obtained from other experimental paradigms, suggest that the $L-M$ and $S-(L+M)$ mechanisms may be separable, yet nonetheless intercorrelated.

2. Methods

2.1. Subjects

Forty-one subjects participated in the factor analysis experiments. All subjects had normal or corrected-

to-normal vision, and normal red/green color vision, as assessed by the *Ishihara Tests for Color Deficiency*. Subject age ranged from 17 to 30 years (mean = 20.6 years, standard deviation = 2.6 years). Three of the subjects from the factor analysis experiment (including the first author) were also tested in a summation-near-threshold experiment.

2.2. Apparatus

Visual stimuli were generated on a Sony Trinitron 500PS monitor (21″ display, 1024 × 768 pixels, 100 Hz refresh) driven by a Cambridge Research Systems (CRS) VSG 2/3 video board. The 15-bit video board allowed for 32,768 discrete luminance levels. The maximum output for the monitor was calibrated to equal-energy white (CIE chromaticity coordinates = 0.333, 0.333), and the voltage/luminance relationship was linearized independently for each of the three guns in the display, using a Gamma Correction System and an OptiCAL 256M (CRS). A PR-650 SpectraColorimeter (PhotoResearch) was used for spectroradiometric and photometric measurements of the stimuli.

2.3. Stimuli

Stimuli consisted of horizontally-oriented sinusoidal gratings, counterphase-reversed (temporal sinusoidal) at 4 Hz. This temporal frequency was chosen because it is in the center of the range tested in our previous factor analysis study, which demonstrated independent $L+M$ and $L-M$ mechanisms (Dobkins et al., 2000). Three different spatial frequencies were employed: 0.25, 0.5, and 1 cycle/degree (c/deg). The main purpose of testing multiple spatial frequencies within each color axis was to increase the number of variables and thus strengthen the factor analysis (see Gorsuch, 1983). Although not intended as such in these experiments, the use of multiple spatial frequencies has the potential to reveal multiple spatial frequency channels. In our experiments, however, we did not observe separate spatial frequency factors, a result that is in line with previous findings from factor analysis studies, at least within the range of spatial frequencies tested in our experiments (see Sekuler et al., 1984; Peterzell & Teller, 1996, 2000; Dobkins et al., 2000). Gratings subtended 5.4° of visual angle, and were convolved with a Gaussian circular envelope (Gabor standard deviation = 2.7°). Gratings were presented with the zero-crossing positioned in the center of the stimulus to ensure equal number of light and dark (or red and green, etc.) stripes in the stimulus. Note that because stimulus size was held constant across all spatial frequencies, the total number of cycles necessarily varied.

Stimuli were modulated along nine directions in color space: the three cardinal axes ($L-M$, $S-(L+M)$, and $L+M$) and six non-cardinal axes (midway between the cardinal axes), all modulated through equal-energy white, at 28 cd/m^2. The $L-M$ gratings were constructed to selectively modulate activity within L- and M-cones, while keeping the S-cone excitation constant. Likewise, the $S-(L+M)$ gratings were constructed to selectively modulate activity in S-cones, while keeping the L- and M-cone excitation constant. $L+M$ gratings modulated all cone types in unison. The six non-cardinal axes were constructed in a "normalized" three-dimensional color space, in which the cardinal axes were scaled to be of equal multiples of thresholds (after Derrington, Krauskopf, & Lennie, 1984; Krauskopf, 1999). (Note that the original Derrington et al. (1984) color space instead scaled cardinal axes to the maximum obtainable on their monitor, and thus their color space was not normalized in this fashion.) Because thresholds can vary across subjects, we tailored color space for each subject by measuring each subject's $L-M$, $S-(L+M)$, and $L+M$ contrast thresholds in a preliminary phase of the experiment. In our color space (shown in Fig. 1), the three cardinal axes can also be referred to by their position in azimuth (A) and elevation (E), where $L-M$ is 0°A, $S-(L+M)$ is 90°A and $L+M$ is 90°E. The six non-cardinal axes employed in this experiment were midway between the cardinal axes and are thus referred to as 45°A, 135°A, 0°A/45°E, 0°A/135°E, 90°A/45°E and 90°A/135°E.

2.4. Paradigm

For all portions of these experiments, subjects were tested in a dark room and viewed the video display binocularly from a chin rest situated 57 cm away. Subjects were instructed to maintain fixation on a small central cross, and provide perceptual reports via keypresses on a response box. For each subject, equiluminance was determined for each chromatic axis in the $(L-M)/(S-(L+M))$ plane via heterochromatic flicker photometry. On each trial, the counterphase grating appeared centered on the fixation cross, and the subject adjusted the relative luminance between the two colors of the grating until the percept of flicker was least salient. For each chromatic axis, an equiluminance point was determined from the mean of 20 trials. This was performed using 0.5 c/deg gratings only, and this setting was used for all three spatial frequencies, since previous studies have shown equiluminance to be stable across spatial frequency (Cavanagh, MacLeod, & Anstis, 1987; Mullen, 1991; Dobkins et al., 2000; Gunther & Dobkins, 2002). When measuring contrast thresholds (see below), chromatic gratings were then presented at each subject's equiluminance setting.

Contrast thresholds were determined for all 27 stimuli (three spatial frequencies by nine color axes) using a Best-PEST staircase procedure (Lieberman & Pentland, 1982) in a spatial two-alternative forced-choice

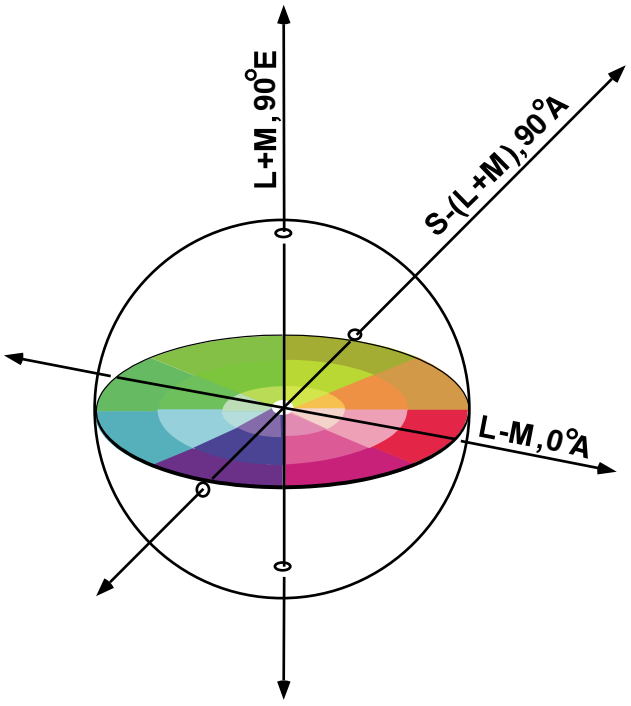

Fig. 1. Depiction of three-dimensional color space. The three cardinal axes are labeled by both their cone computations: $L-M$, $S-(L+M)$ and $L+M$, as well as by their positions in azimuth (A) and elevation (E): 0°A (which appears roughly red/green), 90°A (which appears roughly violet/lime), and 90°E (which appears white/black), respectively. The six non-cardinal axes employed in this experiment are referred to by their position in A and E, as follows: 45°A (which appears roughly purple/chartreuse), 135°A (which appears roughly orange/turquoise), 0°A/45°E (which appears intense-red/dim-green), 0°A/135°E (which appears intense-green/dim-red), 90°A/45°E (which appears intense-violet/dim-lime) and 90°A/135°E (which appears intense-lime/dim-violet).

paradigm. On each trial, the stimulus was centered 2.5° to the left or right of fixation, and the subject reported its location via a key press on a response box. No feedback was provided. Stimuli were presented for 300 ms, with contrast ramped on and off in a cosine manner within the first and last 100 ms. The staircase procedure continued until the subject had completed 125 trials for each stimulus condition. Contrast threshold measurements were divided into three different blocks, each block containing nine of the 27 stimuli (randomly selected). Stimulus presentation was randomized within each block. For each subject, 4–7 h were required to complete the entire experiment, with testing divided into 1.5- to 2-h blocks.

2.5. Factor analyses

Covariance analyses of individual differences (i.e., factor analyses) were performed on the correlations from the contrast threshold data (as previously described, e.g., Peterzell et al., 1995; Peterzell & Teller, 1996; Dobkins et al., 2000) to determine the degree of independence among the nine color axes. Because subject data conformed to normal distributions when log-transformed, all analyses were performed on log values.

As a first step in our factor analysis, a principal component analysis (PCA) was performed on the correlational data. Eigenvalues reflect the proportion of variance explained by a given factor (or component), with 1.0 being the value expected by chance alone. Hence, an eigenvalue greater than 1.0 was used as the criterion for statistical significance of the factors (Guttman, 1954; Gorsuch, 1983). In some cases, we found that the number of statistically significant factors was less than that predicted by our a priori hypothesis. In these instances, we performed two different factor analyses, one based on our a priori hypothesis and one based on the number of factors with significant eigenvalues.

In order to maximize the number of zero or near zero factor loadings, the orthogonal factors resulting from the PCA were rotated to 'simple structure' using the Varimax criterion (Kaiser, 1958), and then further rotated obliquely. Note that the oblique rotation (commonly used in studies of this sort, e.g., Mayer, Dougherty, & Hu, 1995; Dobkins et al., 2000; Peterzell & Teller, 2000) allows for some degree of intercorrelation between factors, which may arise from (1) variation in subjects' overall performance due to cognitive factors (such as attention or motivation) or (2) actual intercorrelation between neural mechanisms underlying the separate factors (e.g., postreceptoral mechanisms could be correlated because they share cone inputs). Either way, the important point is that the factors pulled out in our analyses are meant to reveal regions of color space that are *least* correlated with (i.e., most independent of) one another. Thus, our use of the term "independence" in the context of our factor analysis results is meant to suggest mechanisms that are mostly, although perhaps not entirely, uncorrelated. In addition, note that in all of our factor analyses, we also obtained solutions *without* performing the oblique rotation, and found the results to be nearly identical (although slightly noisier) to those produced by the oblique rotations.

In all of our factor analyses, our criterion for factor loading significance was a value of ± 0.4, which is typical for factor analysis studies (Kline, 1994; Peterzell et al., 1995; Peterzell & Teller, 1996; Dobkins et al., 2000; Gunther & Dobkins, 2002). Note that this 0.4 value is set to be stricter than a criterion for significance based on a Pearson's r value (± 0.31) for the number of subjects (41) in the present study.

Factor analyses were performed on three different configurations of the data. (1) The three cardinal axes (nine total stimuli: three cardinal stimuli by three spatial frequencies). If independent mechanisms underlie detection of the three cardinal axes, a three-factor analysis

is expected to produce factors that load onto each of the axes. (2) Each of the three color planes: $(L-M)/(S-(L+M))$, $(L-M)/(L+M)$, and $(S-(L+M))/(L+M)$ (12 total stimuli per color plane: four color axes by three spatial frequencies). If independent higher-order mechanisms underlie detection of non-cardinal axes, a four-factor analysis is expected to produce factors that load onto each of the four color axes within a color plane (i.e., the two cardinal and the two non-cardinal axes). (3) The entire data set (27 total stimuli: nine color axes by three spatial frequencies). This analysis was performed in order to provide an additional test of independence among all color axes.

2.6. Summation-near-threshold experiments

In order to discern whether the intercorrelation observed between $L-M$ and $S-(L+M)$ in some of our factor analyses could be due to the particular stimulus parameters (e.g., spatial/temporal frequency, stimulus size, duration, etc.) or testing measure (i.e., contrast thresholds) employed, we investigated the separability of the cardinal axes by obtaining contrast thresholds for nearly identical stimuli in a summation-near-threshold paradigm (after Mullen et al., 1997; Mullen & Sankeralli, 1999). This was performed for three subjects, who were also in the factor analysis study. The summation-near-threshold paradigm applies a two-dimensional model to measure the amount of contrast summation occurring between two components embedded in a compound stimulus. Data obtained from this paradigm are often plotted in a *summation square* (see Graham, 1989), where *relative contrast*—the contrast threshold of the component when embedded in the compound, divided by the contrast threshold for that component alone—is plotted for one component on the X-axis and for the other component on the Y-axis.

According to summation theory, when a single mechanism underlies detection of both components, the contrasts of the individual components are expected to add linearly, with the result that the compound stimulus is detected when the relative contrasts of the components sum to 1.0. By comparison, when separable mechanisms underlie detection of the two components, the compound stimulus is detected only when either of the two components is at its respective contrast threshold. In actuality, the separable mechanisms hypothesis predicts relative contrasts slightly below 1.0, because *probability summation* is expected to create a slight advantage for detecting two simultaneously-presented components (i.e., the compound stimulus) over detection of a single component alone (e.g., Watson, Thompson, Murphy, & Nachmias, 1980). Note that because summation is a two-dimensional model, it can only assess the separability of two components. Thus, if a third mechanism exists tuned to, for example, the compound stimulus, this third mechanism would not be revealed by this technique.

The extent of summation between the two component axes can be described by the following equation (based on the vector-magnitude model of Quick (1974)):

$$X^k + Y^k = 1, \tag{1}$$

where X and Y represent relative contrasts of the components. This equation yields values of k near 1.0 for linear summation within a single mechanism, and between 3 and 6 for separable mechanisms with probability summation taken into account.

In our summation set-up, the component stimuli consisted of two (of three) cardinal axes (and thus the compound stimuli were non-cardinal axes in color space). For each of the three planes of color space, $(L-M)/(S-(L+M))$, $(L-M)/(L+M)$, and $(S-(L+M))/(L+M)$, contrast thresholds were obtained for 12 different stimuli: the two cardinal axes plus ten non-cardinal axes spaced 15, 30, 45, 60, and 75° from one of the cardinal axes (total color axes = 33). Data were obtained for 0.5 c/deg, 4 Hz counterphase gratings. As in the factor analysis experiment (*see above*), a normalized color space was created for each subject. All stimuli in the $(L-M)/(S-(L+M))$ color plane (12 total stimuli) were set to be equiluminant for each subject via heterochromatic flicker photometry. Contrast thresholds were measured for all 33 stimuli, randomly divided into four blocks of eight or nine stimuli each.

Optimal k values were calculated for each plane of color space by a least squares error fitting of Eq. (1) to the contrast threshold data from all three subjects simultaneously (thus each k value is based on 30 data points: 5 points by 2 quadrants by 3 subjects). To determine whether these optimal k values were significantly different from 1.0 (i.e., linear summation), we employed a randomization test (Edgington, 1980), in which the randomization distribution of the absolute difference in means of squared error from k = optimal (k_0) and $k = 1.0$ (k_1) was generated using 10,000 random permutations of the sixty values (30 squared errors for k_0 plus 30 squared errors for k_1). The p value was calculated as the number of cases in the randomization distribution that exceeded the observed difference, divided by 10,000.

3. Results

3.1. Factor analyses of cardinal axes

The results from our factor analysis of contrast threshold data obtained for the three cardinal axes, $L-M$, $S-(L+M)$, and $L+M$, are presented in Fig. 2. Shown in Fig. 2A are the factor loadings for a *three*-factor solution on nine data points (three color axes by

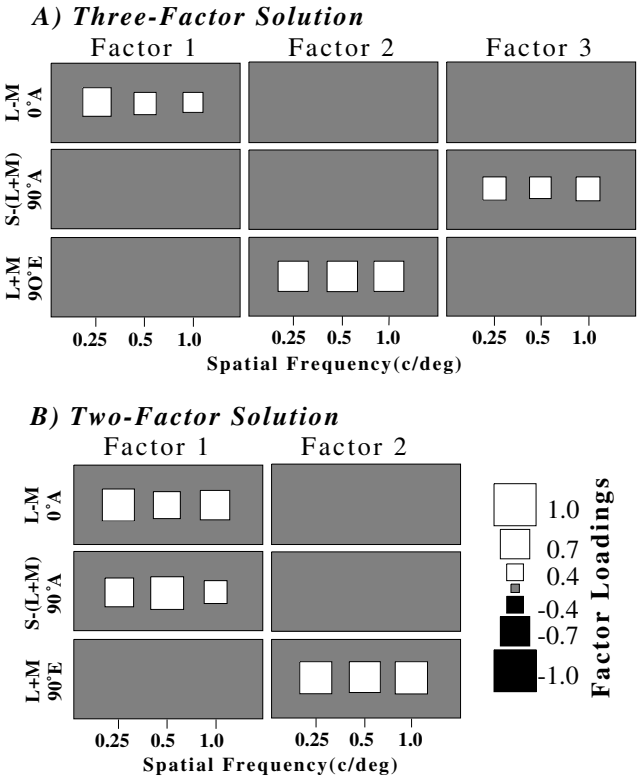

Fig. 2. Factor analysis for the cardinal axes, labeled by both their cone computations: $L-M$, $S-(L+M)$ and L+M, as well as by their position in azimuth (A) and elevation (E): 0°A, 90°A, and 90°E, respectively. Factor loadings, which represent the correlation between the stimulus and the factor, are shown. White and black squares represent positive and negative factor loadings, respectively. Squares are scaled in size according to their value. Only factor loadings that were greater than the criterion for loading significance (factor loading $> |0.4|$) are shown. Positions lacking white or black squares indicate a lack of significant correlation between that stimulus (rows) and that factor (columns). (A) Results of a *three*-factor solution. Here, separate factors are revealed for each of the three cardinal axes. Factor 1 (first column) includes only $L-M$ stimuli, Factor 2 (second column) includes only $L+M$ stimuli, and Factor 3 (third column) includes only $S-(L+M)$ stimuli. (B) Results of a *two*-factor solution. Here, Factor 1 includes *both* $L-M$ and $S-(L+M)$ stimuli and Factor 2 includes only $L+M$ stimuli. This result indicates an intercorrelation between $L-M$ and $S-(L+M)$ mechanisms.

three spatial frequencies), which was chosen based on the hypothesis of independence among the three axes. As described in the methods, our criterion for factor loading significance was a value of 0.4. Thus, only factor loadings with values greater than or equal to $|\pm 0.4|$ are plotted for each of the nine data points. The results of this analysis yielded a highly systematic and interpretable pattern, with independent factors revealed for each of the three cardinal axes. Specifically, $L-M$ stimuli (at all spatial frequencies) loaded onto factor 1 (accounting for 60.1% of the variance), all $L+M$ stimuli loaded onto factor 2 (14.1% of the variance), and all $S-(L+M)$ stimuli loaded onto factor 3 (7.1% of the variance). Consistent with results from previous factor analyses testing spatial frequencies at or below 1 c/deg (Sekuler et al., 1984; Peterzell & Teller, 1996, 2000; Dobkins et al., 2000), the three spatial frequencies in our study (0.25, 0.5, and 1 c/deg) were found to co-load (see Sekuler et al., 1984 for discussion). The correlation matrix underlying all of the factor analyses is provided in the Appendix A.

This pattern of results indicates that different sources of variability underlie the detection of $L-M$, $S-(L+M)$, and $L+M$ contrast, and thus provides evidence for the existence of independent (and separable) mechanisms tuned for the cardinal axes. It is important to point out that this separability is not an artifact of choosing a three-factor solution, as loadings onto the three factors are completely unconstrained in the analysis. Moreover, choosing a greater than three-factor solution had negligible effects on our findings of cardinal axis independence. However, note that only two factors met our criterion for significance based on their eigenvalues (see Section 2). We therefore also performed a two-factor solution, the results of which are shown in Fig. 2B. Here, factor 1 included all $L-M$ and $S-(L+M)$ stimuli (accounting for 60.1% of the variance), while factor 2 included all $L+M$ stimuli (14.1% of the variance). This finding suggests a tendency towards an intercorrelation between $L-M$ and $S-(L+M)$ sensitivity, an issue we return to later in Section 3 and in Section 4.

3.2. Factor analyses of color planes

The results of our factor analyses conducted on contrast threshold values for each of the three color planes, i.e., $(L-M)/(S-(L+M))$, $(L-M)/(L+M)$, $(S-(L+M))/(L+M)$, are presented in Fig. 3. Shown are the factor loadings for *four*-factor solutions on 12 data points per color plane (four color axes by three spatial frequencies). A four-factor solution was chosen based on the hypothesis that higher-order mechanisms underlie detection of non-cardinal axes. Accordingly, each of the four color axes within a color plane (i.e., the two cardinal and the two non-cardinal axes) is expected to load onto a separate factor. Note that in two of the planes, $(L-M)/(L+M)$ and $(S-(L+M))/(L+M)$, exactly four factors were significant based on their eigenvalues. For the $(L-M)/(S-(L+M))$ plane, however, only two factors were significant, and thus both four- and two-factor solutions were performed for this data set.

The $(L-M)/(L+M)$ *plane:* The results of a factor analysis on the $(L-M)/(L+M)$ plane yielded nearly complete segregation of factor loadings for each of the four color axes (Fig. 3, *top panel*). Specifically, all $L-M$ stimuli loaded onto factor 1 (accounting for 37.3% of the variance). All $L+M$ stimuli loaded onto factor 4 (8.6% of the variance). The 0°A/45°E stimuli at 0.25 and 1 c/deg loaded onto factor 3 (11.1% of the variance). All

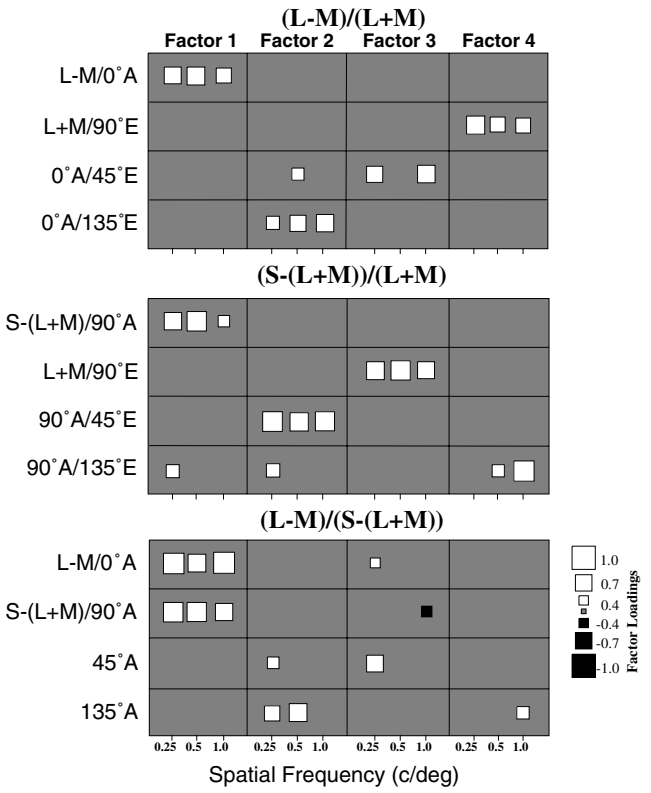

Fig. 3. Factor analyses for each of the three color planes: *Top panel*: $(L-M)/(L+M)$, *middle panel*: $(S-(L+M))/(L+M)$, *bottom panel*: $(L-M)/(S-(L+M))$. Four-factor solutions are shown. Factor loadings and color axis labels are as represented in Fig. 2 (and see Section 2). For both the $(L-M)/(L+M)$ and $(S-(L+M))/(L+M)$ color planes, the four factors load almost exclusively onto each of the four color axes. Results for the $(L-M)/(S-(L+M))$ plane reveal intercorrelation between the $L-M$ and $S-(L+M)$ color axes (see text for details).

0°A/135°E stimuli and one 0°A/45°E stimulus (0.5 c/deg) loaded onto factor 2 (14.1% of the variance).

The $(S-(L+M))/(L+M)$ *plane:* As for the $(L-M)/(L+M)$ plane, the results of a four-factor analysis on the $(S-(L+M))/(L+M)$ plane yielded nearly complete segregation of factor loadings for each of the four color axes (Fig. 3, *middle panel*). All $S-(L+M)$ stimuli and one 90°A/135°E stimulus (0.25 c/deg) loaded onto factor 1 (accounting for 37.3% of the variance). All $L+M$ stimuli loaded onto factor 3 (10.9% of the variance). All 90°A/45°E stimuli and one 90°A/135°E stimulus (0.25 c/deg) loaded onto factor 2 (21.8% of the variance). The 90°A/135°E stimuli at 0.5 and 1 c/deg loaded onto factor 4 (8.3% of the variance).

The $(L-M)/(S-(L+M))$ *plane:* The results of a four-factor solution on the $(L-M)/(S-(L+M))$ plane did not yield segregated factor loadings for each of the four color axes (Fig. 3, *bottom panel*). Instead, factor 1 (43.1% of the variance) included all cardinal stimuli ($L-M$ and $S-(L+M)$) and factor 2 (23.1% of the variance) included 135°A stimuli at 0.25 and 0.5 c/deg and one 45°A stimulus (0.25 c/deg). The remaining two factors did not produce systematic or interpretable loadings. However, because only two factors were significant (based on their eigenvalues), we also applied a two-factor solution to the data set. The results of this analysis yielded one factor that loaded onto both cardinal axes ($L-M$ and $S-(L+M)$, factor 1, accounting for 43.1% of the variance) and another that loaded onto both non-cardinal axes (45°A and 135°A axes, factor 2, accounting for 23.1% of the variance). This common loading for $L-M$ and $S-(L+M)$ stimuli is reminiscent of that observed for the two-factor solution in our analysis of the cardinal axes alone (*above*). We return to the significance of this intercorrelation between $L-M$ and $S-(L+M)$ thresholds in Section 4.

3.3. Factor analysis of all nine color axes

Allowing for the possibility that each color axis tested is independent of the others, we performed a *nine*-factor solution on the entire data set (Fig. 4). Here, only three of the nine factors segregated in a systematic manner. Factor 2 included all $L-M$ and $S-(L+M)$ stimuli (15.5% of the variance). Thus, as noted in our other analyses (*above*), $L-M$ and $S-(L+M)$ stimuli loaded onto a single factor. Factor 4 included all $L+M$ stimuli (6.4% of the variance). Factor 1 (32.5% of the variance) included all 90°A/45°E stimuli. The remaining factors yielded uninterpretable loadings. For this analysis, only seven factors were significant based on their eigenvalues. A *seven*-factor solution was found to be very similar to the nine-factor solution, with $L-M$ and $S-(L+M)$ co-loading onto factor 2 (15.5% of the variance) and $L+M$ loading onto factor 4 (6.4% of the variance). The remaining factors did not exhibit systematic loadings.

One explanation for the lack of systematicity in the nine-axes factor analysis is that we simply did not have enough power to pull out nine independent factors. This is quite possible since our subject:stimuli ratio was rather low in this analysis (1.52, 41 subjects:27 stimuli), which is known to reduce the overall power (see Guadagnoli & Velicer, 1988, and Kline, 1994 for discussion). This is in contrast to our analysis using data from just the three cardinal axes, which had a higher subject:stimuli ratio of 4.56 (41 subjects: 9 stimuli) and yielded highly systematic factors (see Fig. 2). Thus, as the power (subject:stimuli ratio) is reduced, the ability to reveal independent color axes appears to diminish.

3.4. Summation-near-threshold experiments

In several of our factor analyses (*above*), thresholds for $L-M$ and $S-(L+M)$ were found to co-load onto the same factor. These results suggest an intercorrelation between detection of $L-M$ and $S-(L+M)$ stimuli, a finding

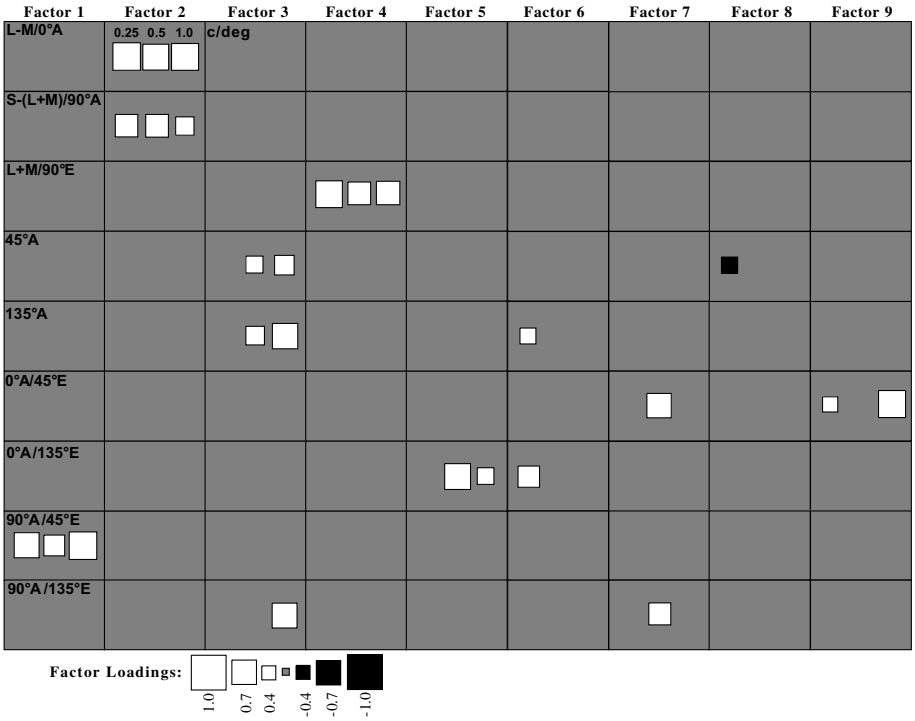

Fig. 4. Nine-factor solution on the entire data set, with factor loadings and color axis labels represented as in Figs. 2 and 3. As for the analysis of the $(L-M)/(S-(L+M))$ color plane (Fig. 3, *bottom panel*), the results for the nine-factor solution reveal an intercorrelation between the $L-M$ and $S-(L+M)$ axes (see text for details).

that seems contradictory to the bulk of the data obtained with other techniques, such as masking, adaptation and summation-near-threshold. In order to ensure that this correlation was not due to our particular stimulus parameters (e.g., spatial/temporal frequency, stimulus size, duration, etc.) or testing measure (i.e., contrast thresholds), we investigated the separability of $L-M$ and $S-(L+M)$ using identical stimuli in a summation-near-threshold paradigm in three subjects. For comparison to data obtained in the $(L-M)/(S-(L+M))$ plane, we also obtained data in the $(L-M)/(L+M)$ and $(S-(L+M))/(L+M)$ color planes.

The results from our summation-near-threshold experiments are presented in summation squares in Fig. 5, where the data for the three subjects have been combined. The results for the $(L-M)/(S-(L+M))$ plane (Fig. 5, *top panel*) yielded a best-fitting k value of 1.7, which was significantly different from the linear summation k value of 1.0 ($p < 0.0001$; dashed diagonal lines in Fig. 5 represent $k = 1$). Thus, in line with previous findings (Mullen & Sankeralli, 1999, mean k across 3 subjects = 2.2), our summation results suggest separability between detection of $L-M$ and $S-(L+M)$ stimuli. Likewise, the $(L-M)/(L+M)$ plane (Fig. 5, *middle panel*) yielded a k value of 3.1, and the $(S-(L+M))/(L+M)$ plane (Fig. 5, *bottom panel*) yielded a k value of 1.9, both of which were significantly different from 1.0 ($(L-M)/(L+M)$: $p < 0.0001$; $(S-(L+M))/(L+M)$: $p = 0.017$), and close to previously reported values ($(L-M)/(L+M)$ color plane: mean k across 5 subjects = 4.0, Mullen et al., 1997; Mullen and Sankeralli, 1999; $(S-(L+M))/(L+M)$ color plane: mean k across 2 subjects = 2.4, Mullen and Sankeralli, 1999). Note, however, that there was a tendency for the 0°E to 90°E quadrant to produce data points near the $k = 1$ line. In fact, when this quadrant was analysed on its own, it yielded a k value of 1.4, which was not significantly different from 1.0 ($p = 0.22$). This result, which implies summation between the $S-(L+M)$ and $L+M$ cardinal axes (within the 0°E to 90°E quadrant), is a bit perplexing since these axes were found to be independent of one another in our factor analyses (see Figs. 2 and 3). It is possible that this result in our summation experiment simply reflects noisy data from these three subjects. Data from additional subjects would be needed to clarify this issue.

In sum, the cardinal axes in all three planes (including $L-M$ and $S-(L+M)$) were shown to be separable via our summation analyses, in accordance with previous studies. For this reason, we believe that the intercorrelation between $L-M$ and $S-(L+M)$ observed in our factor analyses is not a result of the particular stimulus parameters and/or measures employed. Taking the results of the factor analyses and summation-near-threshold experiments together, these findings suggest that $L-M$ and $S-(L+M)$ mechanisms may be separable yet intercorrelated, an issue we return to below.

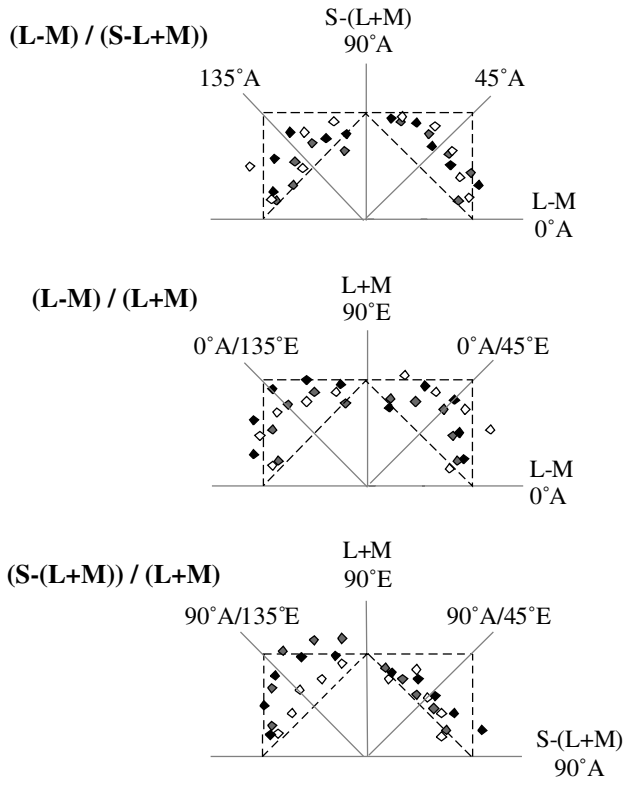

Fig. 5. Data from a summation-near-threshold experiment conducted in three different subjects (black, white and gray diamonds, respectively). *Top panel*: $(S-(L+M))/(L-M)$, *middle panel*: $(L-M)/(L+M)$, *bottom panel*: $(S-(L+M))/(L+M)$. In each color plane, fitted k values are significantly greater than the prediction for linear summation (shown as dashed diagonal line, $k = 1.0$), and thus in line with the notion of separability of the cardinal axes.

4. Discussion

4.1. Mechanisms tuned along the cardinal axes of color space

The results of our three-factor analysis of the cardinal axes revealed separate sources of variability underlying contrast detection of $L-M$, $S-(L+M)$ and $L+M$ stimuli (see Fig. 2A). This result, which suggests the existence of independent mechanisms tuned for the three cardinal axes, is in accordance with those obtained from previous psychophysical studies using techniques such as adaptation, masking, summation-near-threshold, visual search and motion integration (see Section 1). These cumulative psychophysical results are supported by neurophysiological and anatomical studies (in macaque monkeys), which have provided potential neural substrates for the three cardinal axes revealed perceptually. Specifically, neurons within the three main subcortical pathways of the visual system–parvocellular (P), koniocellular (K) and magnocellular (M)–possess color selectivities that map roughly onto the $L-M$, $S-(L+M)$, and $L+M$ axes of color space, respectively (e.g., Derrington et al., 1984; Hendry & Reid, 2000; see Dobkins & Albright, 2003 for a recent review, and Ts'o & Gilbert, 1988 for similar findings within the blobs of V1). This point regarding color selectivity should be qualified, however. Although the different cell types have been shown to exhibit responsitivity to more than one cardinal axis (i.e., *both* M and P neurons respond to *both* $L+M$ and $L-M$ stimuli), they do so with different contrast sensitivities. Specifically, neurons most sensitive to $L+M$ contrast are found within the M pathway, while neurons most sensitive to $L-M$ contrast are found within the P pathway (Croner & Kaplan, 1995; Kaplan & Shapley, 1986; Kremers, Lee, & Kaiser, 1992; Lee, Martin, & Valberg, 1988, 1989; Lee, Martin, Valberg, & Kremers, 1993; Lee, Pokorny, Smith, Martin, & Valberg, 1990; Shapley, 1990; Shapley, Kaplan, & Soodak, 1981). For this reason, it is reasonable to attribute contrast thresholds for $L+M$ and $L-M$ stimuli to the M and P pathways, respectively (e.g., Lee et al., 1990; Smith, Pokorny, Davis, & Yeh, 1995; Dobkins, Anderson, & Lia, 1999; but see Ingling & Martinez-Uriegas, 1983; Lennie & D'Zmura, 1988 for an opposing point of view). Note that although M, P and K neuronal sensitivity to $S-(L+M)$ stimuli has yet to be investigated systematically, the most sensitive neurons are expected to be found within the K pathway. In sum, for experiments employing *threshold* stimuli (as in the present factor analysis), it is highly likely that cardinal stimuli activate one neural pathway in near-isolation of the other two.

Interestingly, although the results from our three-factor analysis of the cardinal axes revealed independence across all three mechanisms tuned along the cardinal axes, we observed intercorrelation between $L-M$ and $S-(L+M)$ contrast thresholds in three other factor analyses: (1) a *two*-factor analysis of the three cardinal axes (Fig. 2B), (2) a factor analysis of the $(L-M)/(S-(L+M))$ color plane (Fig. 3, *bottom panel*), and (3) a factor analysis of all nine color axes (Fig. 4). In all three of these cases, a single factor accounted for the variance in contrast thresholds for $L-M$ and $S-(L+M)$ stimuli. There are several possible explanations for this intercorrelation, which are addressed in turn. The first possibility is that the particular stimulus parameters (e.g., spatial/temporal frequency) or testing measure (i.e., contrast thresholds) we employed were not optimal for revealing separate $L-M$ vs. $S-(L+M)$ mechanisms. Related to this, if our $L-M$ and $S-(L+M)$ chromatic axes were not perfectly orthogonal to one another, this could have resulted in $L-M$ and $S-(L+M)$ stimuli not isolating their respective mechanisms (see Webster, Miyahara, Malkoc, & Raker, 2000). These possibilities seem highly unlikely, however, since the results from our summation-near-threshold experiments, which employed identical stimuli and testing measures, revealed separate $L-M$ and $S-(L+M)$ mechanisms (see Fig. 5, *top panel*).

A second possibility may be that there was not enough power to segregate $L-M$ vs. $S-(L+M)$ stimuli in our factor analyses (i.e., the subject:stimulus ratio was not high enough). Although insufficient power may have contributed to the observed intercorrelation, it is unlikely to account for it in full since, if this were the case, we should have similarly observed intercorrelations between other combinations of the cardinal axes, which we did not.

Alternatively, it is possible that the tendency for intercorrelation between the $L-M$ and $S-(L+M)$ axes revealed in our factor analyses reflects true intercorrelation between the two underlying neural mechanisms. As mentioned in Section 1, the possibility for intercorrelation is not inconsistent with the notion of separability. That is, $L-M$ and $S-(L+M)$ mechanisms may be *separable* (i.e., they can be individually isolated with select stimuli), as revealed in paradigms such as masking, adaptation, and summation-near-threshold, yet the sensitivities of the two mechanisms may nonetheless be intercorrelated, as revealed by factor analysis. At a neuronal level, intercorrelation between separable $L-M$ and $S-(L+M)$ mechanisms could arise if the two mechanisms are influenced by the same gain control mechanism (see Singer & D'Zmura, 1994) and/or are limited by the same source of noise. Peripheral variability, such as that arising from photoreceptor noise (e.g., Vorobyev & Osorio, 1998), is unlikely to account for our results, since this would predict intercorrelation across all color axes (since $L+M$, $L-M$ and $S-(L+M)$ mechanisms share cone inputs), which was not observed in our data. (Note that a similar argument could be made against cognitive factors accounting for our results, since this sort of general factor would also predict intercorrelation across all color axes). Shared variability could, however, exist at the level of the lateral geniculate nucleus (LGN). Recent anatomical studies have shown that K neurons, in addition to forming distinct layers between the M and P layers of the LGN, also form bridges *within* both layers, particularly within the P layers (Hendry & Reid, 2000). Possibly the shared neural environment of P and K neurons arising from these bridges creates a common source of noise or gain control for these two cell types, such that their responses vary in a correlated fashion. Given that P and K neurons underlie $L-M$ and $S-(L+M)$ sensitivity, respectively (see *above*), this could potentially account for the intercorrelation observed psychophysically.

4.2. Higher-order color mechanisms

In addition to addressing the issue of independent cardinal axes, our factor analyses conducted on each of the three color planes allowed us to investigate the existence of independent higher-order mechanisms tuned for *non-cardinal* axes. Here, our results suggest the existence of such mechanisms, at least within the $(L-M)/(L+M)$ and $(S-(L+M))/(L+M)$ color planes, a result that is in line with the bulk of previous psychophysical studies (see Section 1). A potential neural substrate for these higher-order mechanisms comes from neurophysiological studies conducted in visual cortex, which reveal neurons tuned to cardinal, as well as non-cardinal, axes of color space (e.g., Zeki, 1980; Thorell, DeValois, & Albrecht, 1984; Vautin & Dow, 1985; Ts'o & Gilbert, 1988; Lennie, Krauskopf, & Sclar, 1990; Schein & Desimone, 1990; Kiper, Fenstemaker, & Gegenfurtner, 1997; Cottaris & DeValois, 1998; DeValois, Cottaris, Elfar, Mahon, & Wilson, 2000). Although these neural experiments suggest a continuum, rather than discreet classes, of color selectivities in visual cortex, the mere existence of cortical neurons tuned for non-cardinal axes could potentially account for the separability of non-cardinal axes revealed in the present and previous psychophysical studies.

In contrast to the results within the $(L-M)/(L+M)$ and $(S-(L+M))/(L+M)$ color planes, we did not find evidence for mechanisms tuned to higher-order non-cardinal axes within the $(L-M)/(S-(L+M))$ color plane (which may not be surprising given that we also observed intercorrelation between the *cardinal* axes within this plane, *see above*). This latter result is contradictory to the results from previous psychophysical experiments employing adaptation (Krauskopf et al., 1986; Webster & Mollon, 1991, 1994; Krauskopf & Gegenfurtner, 1992), masking (Li & Lennie, 1997), visual search (D'Zmura, 1991; Monnier & Nagy, 2001) and motion coherence (Krauskopf et al., 1996), all of which support the existence of higher-order mechanisms within the $(L-M)/(S-(L+M))$ color plane (but see Webster & Mollon, 1991; Li & Lennie, 1997 for individual differences across subjects).

There are two main possibilities for the apparent discrepancy in the number of mechanisms observed between the present and previous studies. The first possibility concerns differences in results that may be generated from the use of threshold stimuli (which isolate a single, most sensitive, mechanism) vs. suprathreshold stimuli (which may invoke multiple mechanisms). The present factor analysis study employed exclusively threshold stimuli, whereas the aforementioned previous studies used paradigms (i.e., adaptation, masking, visual search, motion coherence) that employ suprathreshold stimuli. (Note that, although adaptation and masking paradigms *measure* thresholds, they nonetheless use suprathreshold stimuli as adapters/masks). This factor is unlikely to account for the discrepancy, however, since threshold experiments would be more likely to isolate separate mechanisms than would suprathreshold experiments, a pattern that is opposite to that observed in the present and aforementioned studies. A second possibility (as mentioned in Section 1, and *above*) concerns the

notion that mechanisms may be *separable* yet nonetheless intercorrelated. Bearing this in mind, detection of non-cardinal axes within the $(L-M)/(S-(L+M))$ color plane may be mediated by separate mechanisms (as suggested by several previous psychophysical studies), however, these mechanisms may share a common source of noise or gain control. Whatever the exact mechanism may be, the results of the present study lead us to predict that neurophysiological studies may reveal correlated noise or common gain control between neurons tuned for different axes within the chromatic, i.e., $(L-M)/(S-(L+M))$, plane of three-dimensional color space.

Acknowledgements

This work was supported by NIH grant EY12153 (KRD). We thank David Peterzell for his many insightful comments on the manuscript and Mark Appelbaum and Larry McClure for statistical consultation.

Appendix A

See Table overleaf. Correlation matrix for the entire data set (nine color axes by three spatial frequencies). Pearson r values are provided. Bold values are negative correlations.

References

Boynton, R. M., Eskew, R. T., & Olson, C. X. (1985). Blue cones contribute to border distinctness. *Vision Research, 25*(9), 1349–1352.

Bradley, A., Switkes, E., & DeValois, K. (1988). Orientation and spatial frequency selectivity of adaptation to color and luminance gratings. *Vision Research, 28*(7), 841–856.

Cavanagh, P., MacLeod, D. I. A., & Anstis, S. M. (1987). Equiluminance: Spatial and temporal factors and the contribution of blue-sensitive cones. *Journal of the Optical Society of America A, 4*(8), 1428–1438.

Cottaris, N. P., & DeValois, R. L. (1998). Temporal dynamics of chromatic tuning in macaque primary visual cortex. *Nature, 395*, 896–900.

Croner, L. J., & Kaplan, E. (1995). Receptive fields of P and M ganglion cells across the primate retina. *Vision Research, 35*(1), 7–24.

Derrington, A. M., Krauskopf, J., & Lennie, P. (1984). Chromatic mechanisms in lateral geniculate nucleus of macaque. *Journal of Physiology, 357*(1), 241–265.

DeValois, R. L., Cottaris, N. P., Elfar, S. D., Mahon, L. E., & Wilson, J. A. (2000). Some transformations of color information from lateral geniculate nucleus to striate cortex. *Proceedings of the National Academy of Sciences, 97*(9), 4997–5002.

Dobkins, K. R., Anderson, C. M., & Lia, B. (1999). Infant temporal contrast sensitivity functions (tCSFs) mature earlier for luminance than for chromatic stimuli: Evidence for precocious magnocellular development? *Vision Research, 39*, 3223–3239.

Dobkins, K. R., Gunther, K. L., & Peterzell, D. H. (2000). What covariance mechanisms underlie green/red equiluminance, luminance contrast sensitive and chromatic (green/red) contrast sensitivity? *Vision Research, 40*, 613–628.

Dobkins, K. R., Stoner, G. R., & Albright, T. D. (1998). Perceptual, oculomotor, and neural responses to moving color plaids. *Perception, 27*, 681–709.

Dobkins K. R., & Albright, T. D., (2003). Merging processing streams: Color cues for motion detection and interpretation. Book Chapter In: L. Chalupa, J. Werner (Eds.), *The visual neurosciences*. MIT Press, Cambridge.

D'Zmura, M. (1991). Color in visual search. *Vision Research, 31*(6), 951–966.

D'Zmura, M., & Knoblauch, K. (1998). Spectral bandwidths for the detection of color. *Vision Research, 38*, 3117–3128.

Edgington, E. E. (1980). *Randomization tests*. New York: Dekker.

Eisner, A., & MacLeod, D. I. A. (1980). Blue sensitive cones do not contribute to luminance. *Journal of the Optical Society of America, 70*, 121–123.

Flanagan, P., Cavanagh, P., & Favreau, O. E. (1990). Independent orientation-selective mechanisms for the cardinal directions of colour space. *Vision Research, 30*(5), 769–778.

Gegenfurtner, K. R., & Kiper, D. C. (1992). Contrast detection in luminance and chromatic noise. *Journal of the Optical Society of America A, 9*(11), 1880–1888.

Giulianini, F., & Eskew, R. T., Jr. (1998). Chromatic masking in the $(\Delta L/L, \Delta M/M)$ plane of cone-contrast space reveals only two detection mechanisms. *Vision Research, 38*, 3913–3926.

Gorsuch, R. L. (1983). *Factor analysis*. Hillsdale: Lawrence Erlbaum Associates.

Graham, N. V. S. (1989). *Visual pattern analyzers*. New York: Oxford University Press.

Guadagnoli, E., & Velicer, W. F. (1988). Relation of sample size to the stability of component patterns. *Psychological Bulletin, 103*(2), 265–275.

Gunther, K. L., & Dobkins, K. R. (2002). Individual differences in chromatic (red/green) contrast sensitivity are constrained by the relative number of L versus M cones in the eye. *Vision Research, 42*(11), 1367–1378.

Gur, M., & Akri, V. (1992). Isoluminant stimuli may not expose the full contribution of color to visual functioning: Spatial contrast sensitivity measurements indicate interaction between color and luminance processing. *Vision Research, 32*, 1253–1262.

Guttman, L. (1954). Some necessary conditions for common-factor analysis. *Psychometrika, 19*(2), 149–161.

Hendry, S. H. C., & Reid, R. C. (2000). The koniocellular pathway in primate vision. *Annual Review of Neuroscience, 23*, 127–153.

Ingling, C. R., & Martinez-Uriegas, E. (1983). The relationship between spectral sensitivity and spatial sensitivity for the primate R^g X-Channel. *Vision Research, 23*, 1495–1500.

Kaiser, H. F. (1958). The Varimax criterion for analytic rotation in factor analysis. *Psychometrica, 23*(3), 187–200.

Kaplan, E., & Shapley, R. M. (1986). The primate retina contains two types of ganglion cells, with high and low contrast sensitivity. *Proceedings of the National Academy of Science USA, 83*(8), 2755–2757.

Kiper, D. C., Fenstemaker, S. B., & Gegenfurtner, K. R. (1997). Chromatic properties of neurons in macaque area V2. *Visual Neuroscience, 14*, 1061–1072.

Kline, P. (1994). *An easy guide to factor analysis*. New York: Routledge.

Kooi, F. L., DeValois, K. K., Switkes, E., & Grosof, D. H. (1992). Higher-order factors influencing the perception of sliding and coherence of a plaid. *Perception, 21*, 583–598.

Krauskopf, J. (1999). Higher order color mechanisms. In K. R. Gegenfurtner & L. T. Sharpe (Eds.), *Color vision: From genes*

Appendix A

	c/deg	*L*−*M*, 0°A			*S*−(*L*+*M*), 90°A			*L*+*M*, 90°E			135°A			45°A			0°A/45°E			0°A/135°E			90°A/45°E			90°A/135°E	
		0.25	0.5	1	0.25	0.5	1	0.25	0.5	1	0.25	0.5	1	0.25	0.5	1	0.25	0.5	1	0.25	0.5	1	0.25	0.5	1	0.25	0.5
L−*M*, 0°A	0.5	0.617																									
	1	0.770	0.713																								
S−(*L*+*M*),	0.25	0.652	0.558	0.693																							
90°A	0.5	0.659	0.592	0.683	0.790																						
	1	0.481	0.522	0.718	0.737	0.643																					
L+*M*,	0.25	0.339	0.353	0.445	0.483	0.334	0.447																				
90°E	0.5	0.499	0.426	0.612	0.445	0.361	0.501	0.665																			
	1	0.261	0.442	0.465	0.497	0.413	0.530	0.611	0.710																		
135°A	0.25	0.093	0.091	0.167	0.255	0.208	0.134	0.142	0.325	0.356																	
	0.5	0.245	0.393	0.318	0.346	0.449	0.338	0.098	0.351	0.507	0.631																
	1	**−0.003**	0.051	0.163	0.060	0.134	0.193	**−0.105**	0.172	0.277	0.579	0.535															
45°A	0.25	0.274	0.054	0.134	0.102	0.170	**−0.129**	**−0.008**	**−0.022**	**−0.089**	0.545	0.351	0.472														
	0.5	0.215	0.363	0.263	0.343	0.354	0.271	0.032	0.129	0.298	0.437	0.554	0.512	0.462													
	1	0.100	0.034	0.214	0.102	0.196	0.205	**−0.031**	0.091	0.092	0.450	0.406	0.649	0.544	0.480												
0°A/45°E	0.25	0.306	0.252	0.343	0.518	0.324	0.313	0.125	0.301	0.424	0.581	0.464	0.358	0.321	0.428	0.248											
	0.5	0.278	0.118	0.293	0.229	0.175	0.124	0.180	0.280	0.338	0.124	0.200	0.160	0.272	0.377	0.209	0.192										
	1	0.044	0.180	0.208	0.201	0.000	0.263	0.084	0.360	0.348	0.351	0.340	0.301	0.014	0.284	0.115	0.408	0.291									
0°A/135°E	0.25	0.280	0.165	0.224	0.291	0.323	0.127	0.045	0.113	0.136	0.426	0.302	0.190	0.451	0.430	0.336	0.424	0.315	0.068								
	0.5	0.270	0.026	0.289	0.168	0.188	0.167	0.034	0.296	0.091	0.342	0.315	0.378	0.281	0.341	0.300	0.221	0.275	0.240	0.359							
	1	0.311	0.104	0.325	0.280	0.263	0.276	0.200	0.204	0.147	0.308	0.120	0.257	0.163	0.252	0.475	0.195	0.298	0.046	0.356	0.385						
90°A/45°E	0.25	0.032	**−0.074**	0.055	0.079	0.027	**−0.047**	0.174	**−0.041**	0.002	0.371	0.126	0.314	0.551	0.425	0.404	0.191	0.258	**−0.033**	0.375	0.228	0.354					
	0.5	0.154	**−0.005**	0.117	**−0.010**	0.039	**−0.081**	0.022	0.221	0.128	0.430	0.266	0.484	0.448	0.324	0.419	0.281	0.324	0.065	0.353	0.379	0.521	0.638				
	1	**−0.091**	**−0.045**	0.123	0.051	0.016	0.024	0.138	0.050	0.165	0.347	0.053	0.318	0.299	0.165	0.281	0.249	0.406	0.153	0.371	0.057	0.391	0.637	0.561			
90°A/	0.25	0.389	0.291	0.449	0.468	0.540	0.296	0.116	0.105	0.227	0.353	0.403	0.450	0.621	0.605	0.515	0.387	0.423	**−0.025**	0.544	0.257	0.435	0.569	0.515	0.448		
135°E	0.5	0.257	0.062	0.327	0.281	0.328	0.364	0.191	0.174	0.271	0.234	0.269	0.358	0.324	0.504	0.416	0.068	0.507	0.162	0.423	0.384	0.514	0.281	0.336	0.302	0.535	
	1	0.118	0.109	0.307	0.202	0.124	0.414	0.083	0.185	0.299	0.401	0.426	0.607	0.264	0.475	0.360	0.325	0.074	0.313	0.081	0.287	0.200	0.308	0.271	0.151	0.335	0.424

to perception (pp. 304–316). Cambridge: Cambridge University Press.

Krauskopf, J., & Gegenfurtner, K. (1992). Color discrimination and adaptation. *Vision Research, 32*(11), 2165–2175.

Krauskopf, J., Williams, D. R., & Heeley, D. W. (1982). Cardinal directions of color space. *Vision Research, 22*, 1123–1131.

Krauskopf, J., Williams, D. R., Mandler, M. B., & Brown, A. M. (1986). Higher order color mechanisms. *Vision Research, 26*(1), 23–32.

Krauskopf, J., Wu, -J., & Farell, B. (1996). Coherence, cardinal directions, and higher-order mechanisms. *Vision Research, 36*(9), 1235–1245.

Kremers, J., Lee, B. B., & Kaiser, P. K. (1992). Sensitivity of macaque retinal ganglion cells and human observers to combined luminance and chromatic temporal modulation. *Journal of Optical Society of America A, 9*(9), 1477–1485.

Lennie, P., Krauskopf, J., & Sclar, G. (1990). Chromatic mechanisms in striate cortex of macaque. *The Journal of Neuroscience, 10*(2), 649–669.

Lennie, P., & D'Zmura, M. (1988). Mechanisms of color vision. *Critical reviews in neurobiology, 3*, 333–400.

Li, A., & Lennie, P. (1997). Mechanisms underlying segmentation of colored textures. *Vision Research, 37*(1), 83–97.

Lieberman, H. R., & Pentland, A. P. (1982). Microcomputer-based estimate of psychophysical thresholds: The Best PEST. *Behavioral Research Methods and Instrumentation, 14*(1), 21–25.

Lee, B. B., Martin, P. R., & Valberg, A. (1988). The physiological basis of heterochromatic flicker photometry demonstrated in the ganglion cells of the macaque retina. *Journal of Physiology (London), 404*(323), 323–347.

Lee, B. B., Martin, P. R., & Valberg, A. (1989). Sensitivity of macaque retinal ganglion cells to chromatic and luminance flicker. *Journal of Physiology (London), 414*, 223–243.

Lee, B. B., Martin, P. R., Valberg, A., & Kremers, J. (1993). Physiological mechanisms underlying psychophysical sensitivity to combined luminance and chromatic modulation. *Journal of Optical Society of America A, 10*(6), 1403–1412.

Lee, B. B., Pokorny, J., Smith, V. C., Martin, P. R., & Valberg, A. (1990). Luminance and chromatic modulation sensitivity of macaque ganglion cells and human observers. *Journal of Optical Society of America A, 7*(12), 2223–2236.

Mayer, M. J., Dougherty, R. F., & Hu, L.-T. (1995). A covariance structure analysis of flicker sensitivity. *Vision Research, 35*(11), 1575–1583.

Monnier, P., & Nagy, A. L. (2001). Uncertainty, attentional capacity and chromatic mechanisms in visual search. *Vision Research, 41*(3), 313–328.

Mullen, K. T. (1991). Colour vision as a post-receptoral specialization of the central visual field. *Vision Research, 31*, 119–130.

Mullen, K. T., Cropper, S. J., & Losada, M. A. (1997). Absence of linear subthreshold summation between red–green and luminance mechanisms over a wide range of spatio-temporal conditions. *Vision Research, 37*(9), 1157–1165.

Mullen, K. T., & Losada, M. A. (1994). Evidence for separate pathways for color and luminance detection mechanisms. *Journal of the Optical Society of America A, 11*, 3136–3151.

Mullen, K. T., & Losada, M. A. (1999). The spatial tuning of color and luminance peripheral vision measured with notch filtered noise masking. *Vision Research, 39*, 721–731.

Mullen, K. T., & Sankeralli, M. J. (1999). Evidence for the stochastic independence of the blue–yellow, red–green and luminance detection mechanisms revealed by subthreshold summation. *Vision Research, 39*, 733–745.

Peterzell, D. H., & Teller, D. Y. (1996). Individual differences in contrast sensitivity functions: The lowest spatial frequency channels. *Vision Research, 36*(19), 3077–3085.

Peterzell, D. H., & Teller, D. Y. (2000). Spatial frequency tuned covariance channels for red–green and luminance-modified gratings: Psychophysical data from human adults. *Vision Research, 40*, 417–430.

Peterzell, D. H., Werner, J. S., & Kaplan, P. S. (1993). Individual differences in contrast sensitivity functions: The first four months of life in humans. *Vision Research, 33*(3), 381–396.

Peterzell, D. H., Werner, J. S., & Kaplan, P. S. (1995). Individual differences in contrast sensitivity functions: Longitudinal study of 4-, 6-, and 8-month-old human infants. *Vision Research, 35*(7), 961–979.

Quick, R. F., Jr. (1974). A vector-magnitude model of contrast detection. *Kybernetik, 16*, 65–67.

Sankeralli, M. J., & Mullen, K. T. (1997). Postreceptoral chromatic detection mechanisms revealed by noise masking in three-dimensional cone contrast space. *Journal of the Optical Society of America A, 14*(10), 2633–2646.

Schein, S. J., & Desimone, R. (1990). Spectral properties of V4 neurons in the macaque. *The Journal of Neuroscience, 10*(10), 3369–3389.

Sekuler, R., Wilson, H. R., & Owsley, C. (1984). Structural modeling of spatial vision. *Vision Research, 24*(7), 689–700.

Shapley, R. (1990). Visual sensitivity and parallel retinocortical channels. *Annual Review of Psychology, 41*, 635–658.

Shapley, R., Kaplan, E., & Soodak, R. (1981). Spatial summation and contrast sensitivity of X and Y cells in the lateral geniculate nucleus of the macaque. *Nature, 292*(5823), 543–545.

Singer, B., & D'Zmura, M. (1994). Color contrast induction. *Vision Research, 34*(23), 3111–3126.

Smith, V. C., Pokorny, J., Davis, M., & Yeh, T. (1995). Mechanisms subserving temporal modulation sensitivity in silent-cone substitution. *Journal of Optical Society of America A, 12*(2), 241–249.

Stockman, A., MacLeod, D. I. A., & DePriest, D. D. (1991). The temporal properties of the human short-wave photoreceptors and their associated pathways. *Vision Research, 31*, 189–209.

Switkes, E., Bradley, A., & DeValois, K. K. (1988). Contrast dependence and mechanisms of masking interactions among chromatic and luminance gratings. *Journal of the Optical Society of America A, 5*(7), 1149–1162.

Thorell, L. G., DeValois, R. L., & Albrecht, D. G. (1984). Spatial mapping of monkey V1cells with pure color and luminance stimuli. *Vision Research, 24*(7), 751–769.

Ts'o, D. Y., & Gilbert, C. D. (1988). The organization of chromatic and spatial interactions in the primate striate cortex. *The Journal of Neuroscience, 8*(5), 1712–1727.

Vautin, R. G., & Dow, B. M. (1985). Color cell groups in foveal striate cortex of the behaving macaque. *Journal of Neurophysiology, 54*(2), 273–292.

Vorobyev, M., & Osorio, D. (1998). Receptor noise as a determinant of colour threshold. *Proceedings of the Royal Society of London B, 265*, 351–358.

Watson, A. B., Thompson, P. G., Murphy, B. J., & Nachmias, J. (1980). Summation and discrimination of gratings in opposite directions. *Vision Research, 20*, 341–347.

Webster, M. A., & MacLeod, D. I. A. (1988). Factors underlying individual differences in the color matches of individual observers. *Journal of the Optical Society of America A, 5*(10), 1722–1735.

Webster, M. A., Miyahara, E., Malkoc, G., & Raker, V. E. (2000). Variations in normal color vision. I. Cone-opponent axes. *Journal of the Optical Society of America A, 17*(9), 1535–1544.

Webster, M. A., & Mollon, J. D. (1991). Changes in colour appearance following post-receptoral adaptation. *Nature, 349*, 235–238.

Webster, M. A., & Mollon, J. D. (1994). The influence of contrast adaptation on color appearance. *Vision Research, 34*(15), 1993–2020.

Zeki, S. M. (1980). The representation of colours in the cerebral cortex. *Nature, 284*, 412–418.